Draft version, Nov. 11, 2008

ROYAL INSTITUTE
OF TECHNOLOGY

Bioaccessibility studies of silver and silver compounds in synthetic biological media

Klara Midander, Inger Odnevall Wallinder✉
Div. Corrosion Science, Dep. Chemistry, School of Chemical Sciences and Engineering,
Royal Institute of Technology, KTH
Drottning Kristinas väg 51, SE-100 44 Stockholm, Sweden

Commissioned by
EBRC, GmbH

✉ ingero@kth.se
☎ + 46 8 790 66 21
💻 www.corrosionscience.se

Executive summary

Bioaccessibility data on silver released from commercially available silver metal powder, silver oxide particles and silver nitrate particles have been generated when exposed to synthetic biological media of varying pH and composition. The following main conclusions are drawn:

- The BET area of the investigated test materials varied from 0.03 to 3.1 m^2/g with particle distributions from 0.07 to 62 μm sized particles (median values, volume %). According to XPS measurements the surface of the metallic silver particles was covered or partially covered by a few nanometer thick layer of silver oxide. In addition, these particles revealed strongly oxidized carbon components on the surface. Their origin is not believed to originate from atmospheric contamination.
  Particles of silver oxide and silver nitrate showed the presence of an oxidized silver surface and the presence of nitrate, respectively, without any significant presence of oxidized carbon species.

- Most silver was released/dissolved during the first 2 hours of exposure in all media investigated. The released silver concentrations from all test materials were highest in phosphate buffered saline (PBS), having a neutral pH but the highest chloride content of the test media investigated. Released silver concentrations were lowest in artificial gastric fluid (GST) having the most acidic pH and the lowest concentration of chlorides of the test media investigated.

- The release rate of silver decreased according to the following sequence for all samples investigated after 2 hours of exposure:

  PBS > GMB > ASW > ALF >> GST

  This sequence is in agreement with decreasing chloride concentration in the different test media investigated:

  PBS (5.35 g/L) > GMB (3.97 g/L) > ASW (3.05 g/L) > ALF (2.02 g/L) > GST (0.97g/L).

- Less than 0.5% of the particle mass was dissolved after 24 hours of exposures in all media for all test materials investigated.

Background

Human exposure to particulate matter in our daily environment has become an issue of increased interest. The exposure may relate, for example, to certain occupational activities or to vehicular emissions; and the composition of particles varies over a broad range and may often include metallic materials and metal compounds. The potential for adverse effects on human health due to exposure, for example through inhalation and/or ingestion of metal particles or metal compounds and following the release of metal ions needs further investigation.

To obtain reproducible data in terms of metal ion release from particles exposed to a test media, many factors need to be taken into account:

- Particle size and distribution of the powder material determine the surface area, which is important in terms of quantifying the amount of released metal ions.
- The surface area is important for the selection of a relevant ratio between the surface area and the solution volume. It is also important if the metal release is to be presented in relation to the surface area, for example in units of $\mu g/cm^2$/hour. It is difficult to assess the true surface area (total area considering roughness porosity etc.) and the active area fraction taking part in the corrosion/dissolution process. The specific surface area is a measurable quantity that can be used as an approximation of the surface area.
- The shape of particles may have an influence on the metal release process since sharp edges are usually more prone to dissolution.
- Knowledge of the type of metal compound and its respective dissolution characteristics are crucial for accurate interpretation and comparison of results.
- Since it is impractical or even impossible to clean the particles under investigation, their surface condition should be characterized with surface sensitive techniques, for example x-ray photoelectron spectroscopy (XPS) prior to exposure.
- During exposure, the particles should be suspended in the solution and therefore the need for standardised stirring conditions should be taken into account. If this parameter is not considered, the effective surface area will be unknown and dissolution data irrelevant.
- Before solution analysis, the particles must be removed from the test solution. Therefore, separation techniques should be used that ensure that no particles remain in the solution.

Thus, it is clear that, to obtain accurate, meaningful and relevant results, suitable test procedures and experience in handling different powder particles are essential for the measurement of metal release from different types of metal compounds.

Overall aim

The aim of this research project is to generate quantitative bioaccessibility data for silver metal powder of a commercially available size compared to silver oxide particles and silver nitrate particles exposed to different synthetic biological media. Generated results form a unique set of data to be used for further investigations of possible toxic effects that could arise from exposure of such particles. In parallel, the particles have been physically and chemically characterized by determining the specific surface area, the particle size distribution, particle morphology and surface oxide composition. An improved understanding of particle characteristics and its reactivity in synthetic biological fluids can be utilised in order to assist in determining the relative health risks associated with inhalation or ingestion of silver and silver containing particles.

Materials and methods

Test materials

Two pure silver powders together with silver oxide and silver nitrate particles were studied:

(I) silver metal powder, Batch PMC 2, denoted Ag-1 in the following

Substance name:	silver
CAS No:	7440-22-4
Molecular formula:	Ag
Moelcular weight:	107.87 g/mol
Appearance:	metallic powder
Purity:	99.2 % (stated by the producer)
Storage:	closed container, cool, dry, ventilated area
Stability:	nominal shell life 365 days (at least until March 2009)
Water solubility:	considered "insoluble"
Relative density:	10.5 (MSDS provided by the producer)
Tapped density:	3.20 g/cm^3 (stated by the producer)
Surface area:	3.0 m^2/g (stated by the producer)
Particle size:	volume based particle size distribution (provided by the producer)
	D_{10}: 0.8 µm
	D_{50}: 1.9 µm
	D_{90}: 11.2 µm

(II) silver metal powder, Batch PMC 3 (very fine, nanometer range), denoted Ag-2

Substance name:	silver
CAS No:	7440-22-4
Molecular formula:	Ag
Moelcular weight:	107.87 g/mol
Appearance:	metallic powder
Purity:	min 98 % (stated by the producer)
Storage:	closed container, cool, dry, ventilated area
Stability:	a chemical modification is not anticipated during storage, the powder particles may agglomerate
Water solubility:	considered "insoluble"
Relative density:	10.5 (MSDS provided by the producer)
Tapped density:	2.7 g/cm^3 (stated by the producer)
Surface area:	11.04 m^2/g (stated by the producer)
Particle size:	volume based particle size distribution (provided by the producer)
	D_{10}: 20 nm
	D_{50}: 35 nm
	D_{90}: 60 nm

(III) disilver oxide powder (Ag_2O), Batch PMC 1, denoted Ag_2O

Substance name:	disilver oxide
CAS No:	20667-12-3
Molecular formula:	Ag_2O
Moelcular weight:	231.74 g/mol
Appearance:	solid, light coloured
Purity:	93.7 % (stated by the producer), corresponds to > 99.9 % Ag_2O
Storage:	tightly closed container in cool, well ventilated area, separate from acids, alkalis, reducing agents and combustibles
Stability:	until March 2009
Water solubility:	"insoluble in hot or cold water"
Relative density:	7.14 g/cm^3 (20°C) (stated by the producer)
Tapped density:	1.32 g/cm^3 (stated by the producer)
Surface area:	0.32 m^2/g (stated by the producer)
Particle size:	volume based particle size distribution (provided by the producer)
	D_{10}: 2.2 µm
	D_{50}: 3.9 µm
	D_{90}: 6.8 µm

(III) silver nitrate crystals ($AgNO_3$), Batch PMC 1, denoted $AgNO_3$

Substance name:	silver nitrate
CAS No:	7761-88-8
Molecular formula:	$AgNO_3$
Moelcular weight:	169.87 g/mol
Appearance:	white crystalline
Purity:	min 99.9 % $AgNO_3$ (stated by the producer)
Storage:	tightly closed container, avoid light effect and humidity, product has a corrosive effect on aluminium or steel
Stability:	no expiration date if product is kept on original package
Water solubility:	approx. 2.16 kg/L (20°C) (stated by the producer)
Relative density:	approx. 4.35 g/cm^3 (stated by the producer)
Surface area:	0.15 m^2/g (stated by the producer)
Particle size:	volume based particle size distribution (provided by the producer)
	D_{10}: 231 µm
	D_{50}: 367 µm
	D_{90}: 486 µm

The test materials were supplied to KTH by EBRC Consulting GmbH. A quantity of 200 g was provided for each test substance.

Particle characterization

Information on silver content, powder density and particle size distribution data were provided by EBRC Consulting GmbH. Further characterisation of the specific surface area, the particle size distribution in a relevant solution, the surface composition and morphology of the silver powders was performed by the Division of Corrosion Science, KTH.

Specific surface area of all particles was determined by means of BET analysis (Brunauer, Emmett, Teller), using a Micromeritics Gemini V instrument. The surface area of a particulate sample with known mass is estimated via the adsorption of nitrogen at cryogenic conditions, knowing the amount of nitrogen atoms adsorbed on the surface of the particles and the size of nitrogen atoms.

Particle size distributions in phosphate buffered saline, PBS, were measured by laser diffraction technique using a Malvern Mastersizer 2000 equipment with a Hydro SM dispersion unit. The instrumental software uses the Mie theory to predict the particle size as the diameter of the "equivalent sphere" which gives the same light scattering response (with the intensity predicted by the refractive index difference between the particle and the dispersion media) as the particles being measured. Refractive indexes for Ag or $AgNO_3$ and water (since it is the solvent for the test media) were used as input parameters for the size measurements. Standard operational conditions were applied for the measurements.

Surface compositional analyses were performed using x-ray photoelectron spectroscopy, XPS. Spectra were recorded using a Kratos AXIS UltraDLD x-ray photoelectron spectrometer (Kratos Analytical, Manchester, UK) using a monochromatic Al x-ray source (150 W) on areas approximately sized 700 x 300 μm. Wide spectra were run to detect elements present in the surface layer. Relative surface compositions were obtained from quantification of high resolution (20 eV pass energy) detailed spectra for carbon, oxygen, nitrogen and silver. Oxygen carbon and silver spectra were curve-fitted showing chemical shifts for each element.
The powder samples were fixed on copper tape to avoid any dispersion of powder particles in vacuum inside the instrument chamber. All binding energies were calibrated by assigning the carbon C1s contamination peak to 285.0 eV. All peak areas were determined by assigning a linear base line.

Backscattered electron images of the silver metal, silver oxide and silver nitrate particles were generated using Scanning Electron Microscopy, SEM (Hitachi TM-1000). The powder samples were fixed on carbon tape to avoid any dispersion of powder particles in vacuum inside the instrument chamber and to assure appropriate conduction.

Bioaccessibility studies

Test Media

The silver metal, silver oxide and silver nitrate particles were exposed to five different test media separately at a pH range from about 4.5 to 7.4. The test media were:

- *Gamble's solution* (GMB, pH 7.4) which mimics interstitial fluid within the deep lung under normal health conditions (Stopford et al, 2004).
- *Phosphate-buffered saline* (PBS, pH 7.4), is a standard physiological solution that mimics the ion strength of human blood serum. It is widely used in the research (e.g. Norlin et al, 2002) and medical health care community (e.g. Hanawa et al, 2004; Okazaki and Gotoh, 2004) as a reference test solution for comparison of data under simulated physiological conditions.
- *Artificial sweat* (ASW, pH 6.5) simulates the hypoosmolar fluid, linked to hyponatraemia (loss of Na+ from blood), which is excreted from the body when sweating. The fluid is recommended in the available standard for testing of nickel release from nickel containing products (EN1811, 1998).
- *Artificial lysosomal fluid* (ALF, pH 4.5), which simulates intracellular conditions in lung cells occurring in conjunction with phagocytosis and represents relatively harsh conditions (Stopford et al, 2004).
- *Artificial gastric fluid* (GST, pH 1.5) mimics the very harsh digestion milieu of high acidity in the stomach. (ASTM D5517)

The test media were selected to simulate relevant inhalation scenarios (as far as practical) where silver metal, silver oxide or silver nitrate particles may enter the human body through inhalation and, subsequently by ingestion of inhaled particles that are translocated to the gastro-intestinal tract. It should be stressed though, that the different test media only simulate physiological conditions to a limited extent, for example, citrate in Gamble's solution replaces proteins and acetate is added to represent organic acids (Kuhn and Rae, 1988; Moss, 1979; Stopford et al, 2003) as the complexity and function of the real body fluids are difficult to simulate. However, *in vitro* results in such synthetic biological media can, in a simple way, provide information that could be relevant for a real situation. Experience and capability in preparation and handling of the test solutions has been gained over the last ten years at the Division of Corrosion Science, Royal Institute of Technology (KTH) (e.g. Herting et al, 2006a; Herting et al, 2006b; Midander et al, 2007).

The test solutions were prepared using ultra-pure water and chemicals of analytical grades. All vessels used were acid-cleaned (10% HNO_3 for at least 24 hours, rinsed four times with ultra-pure water and dried in ambient air in the laboratory) to avoid any risk of contamination.
The chemical composition (g/L) of ALF and GMB are compiled in Table I and the composition of ASW, PBS and GST in Table II. The pH of ALF and GMB was adjusted using 50% NaOH and 25% HCl respectively. The pH of PBS was adjusted with 50% NaOH. For ASW, the pH was adjusted using 1% dilute ammonia solution

Table I. Composition [g/L] and pH of ALF and GMB.

Chemical	**ALF**	**GMB**
$MgCl_2$	0.0497	0.0953
NaCl	3.210	6.0193
KCl	-	0.2982
Na_2HPO_4	0.071	0.126
Na_2SO_4	0.039	0.063
$CaCl \cdot 2H_2O$	0.128	0.3676
$C_2H_3O_2Na \cdot H_2O$ (Sodium acetate)	-	0.7005
$NaHCO_3$	-	2.6043
NaOH	6.000	-
Citric acid	20.80	-
Glycine	0.059	-
$C_6H_5Na_3O_7 \cdot 2H_2O$ (Na_3Citrate $\cdot 2H_2O$)	0.077	0.097
$C_4H_4O_6Na_2 \cdot 2H_2O$ (Na_2Tartrate $\cdot 2H_2O$)	0.090	-
$C_3H_5NaO_3$ (NaLactate)	0.085	-
$C_3H_5O_3Na$ (NaPyruvate)	0.086	-
pH	**4.5**	**7.4**

Table II. Composition [g/L] and pH of ASW, PBS and GST

Chemical	**ASW**	**PBS**	**GST**
NaCl	5.00	8.77	-
Na_2HPO_4	-	1.28	-
$NaHCO_3$	-	-	-
NaOH	-	-	-
KCl	-	-	-
KH_2PO_4	-	1.36	-
$CaCl_2 \cdot 2H_2O$	-	-	-
Urea	1.00		-
Lactic acid	1.00		-
HCl	-	-	1.0
pH	**6.5**	**7.2-7.4**	**1.5-1.6**

Experimental Procedure

Triplicate powder samples were prepared for exposure in the different test media, each for two time periods. In addition, one blank sample (without addition of any test material) containing only the test solution was incubated together with the triplicates for each time period. 5 ± 0.5 mg of the test material was weighed using a Mettler AT20 balance with readability of 2 μg, and placed in a TPX Nalge® jar. 50 mL of the test solution was then added to the TPX Nalge® jar containing the powder sample, before incubated at dark conditions in a Stuart shaker incubator S180 regulated at 37 ± 0.5°C. The solution was gently shaken (bi-linearly) with an intensity of 25 cycles per minute (no adjustment of solution volume to powder mass was made). The testing periods were 2 and 24 hours. After the testing period, the samples were allowed to cool down to ambient room temperature before the final pH of the test solution was measured. The test medium was then separated from the powder particles by centrifugation at 3000 rpm for 10 minutes, resulting in a visually clear supernatant with remaining particles in the bottom of the centrifuging tube. In some cases fine particles were floating on the solution surface after centrifugation. These particles were removed using acid cleaned pasteur pipettes. The supernatant solution was decanted into a LDPE storage flask and acidified to pH <2 with 65% pure HNO_3 prior to solution analysis (a standard procedure for metal analysis). All vessels for exposure, centrifugation and storage of samples were acid-cleaned in 10% HNO_3 for at least 24 hours, then rinsed four times with ultra-pure water and dried in ambient air in the

laboratory, to avoid any risk of contamination.

The particle loading of 0.1 g/L (corresponding to 5 mg of the test material per 50 mL volume of solution) was selected since it is experimentally feasible even when low concentrations of released metal are expected. The particle loading chosen for exposures can always be discussed in the context of its relevance but the reasoning about this is not straightforward. For example, the real deposition of particles in the human lung when inhaled is dependent on several factors such as particle concentration in the air, size of particles and respiratory intensity. Also the site of deposition depends on these factors and at specific "hot spots" the total amount of particles deposited may locally become relatively high (Martonen, 1992a; Martonen et al, 1992b; Miki et al, 1992; Balashazy et al, 2003).

The particle loading is a very important parameter which is intimately related to the surface area per volume ratio, and crucial for the prediction/comparison of metal release data from particles. Since surface area increases dramatically with smaller particle dimensions, the use of small particles and large volumes drives the transformation/dissolution equilibrium towards higher total release. Moreover, the risk for agglomeration of particles, and hence a reduced, uncontrolled surface area of particles, is enhanced with a high particle loading especially if inadequate appropriate mixing/agitation is provided (Midander et al, 2006). This would lead to a reduced release of metal ions.

The time periods for the exposure of the silver metal, silver oxide and silver nitrate particles, 2 hour and 24 hours respectively, were selected to have some relevance to the inhalation/ingestion scenario and to enable comparison with other metal ion release/dissolution data generated for these time periods. The approximate time for the gastric phase of digestion is about 2 hours, and therefore this exposure time period was considered relevant for testing in artificial gastric fluid (Hamel et al, 1998). The 24 hour exposure was selected as a standard time duration that is relatively easy to compare with existing metal ion release/dissolution data as well as toxicity data for further evaluation of the bioaccessibility of released silver.

Metal analysis

The silver concentrations of the solution samples where analysed by atomic absorption spectroscopy (AAS) using the oxidising air/acetylene-flame. The standard method for silver analysis developed for the instrument (Perkin Elmer AAnalyst 800) was followed using calibration standards of concentration 1, 3 and 10 mg/L. A calibration correlation coefficient of 1.000 was accepted for the analysis that was performed at the wavelength of 328.1 nm having the highest sensitivity for silver. The detection limit (3*STD of blank sample) was less than 6 μg/L for all of the test solutions (matrixes). The silver concentration results were based on triplicate readings of each solution sample. Quality control samples were analysed consecutively.

Results and discussion

Particle characterisation - surface area, particle size distribution and morphology

The surface area of the different test materials was determined by means of BET analysis (adsorption of nitrogen atoms on the particle surface at cryogenic conditions - a measure of specific surface area), see Table III.

Morphology observations of the test materials using scanning electron microscopy, SEM, are displayed in Figure 1.

To investigate the behaviour of the silver metal, silver oxide and silver nitrate particles when dispersed in a relevant test solution, the size distribution was determined when immersed in phosphate buffered saline (PBS) by means of laser diffraction. Measurements of the particle size distribution in solution are conducted when dispersed particles are continuously pumped through the laser diffraction system. The results reflects the stability of possible clusters formed due to aggregation/agglomeration (that are formed in air but still are present when dispersed in solution).The measured median particle size ($d_{0.5}$) is compiled in Table III together with 10% ($d_{0.1}$) and 90% ($d_{0.9}$) percentile values as the percentage in volume (mass), relevant for micron sized particles, and the percentage in number, more relevant for nano sized particles (since nano particles have a very small volume). The results are described as the average value of three replicate measurements. The median particle diameter is also graphically illustrated in Figure 2.

The silver metal powder, Ag-1, shows a broad particle size distribution that contains a fraction of smaller sized particles (< 0.1 μm in diameter, better represented in number%) see Figure 2. The silver particles show a fairly rough surface structure that contributes to the relatively large specific surface area, 3.1 m^2/g, measured by BET analysis. The other silver metal powder tested, Ag-2, has a completely different appearance and surface morphology, just like "fine gravel" as seen from SEM images, Figure 1. Similar to the other silver powder, the Ag-2 particles show a broad distribution in size, including a large fraction of smaller sized particles and a large specific surface area of 7.9 m^2/g. Silver oxide particles, Ag_2O, seem to consist of larger agglomerates of finer, spherical silver oxide particles. The particles are all of similar size range and if the particles consist of agglomerated finer oxide particles, they are very stable since they do not fall apart when agitated during the size distribution analysis (this is seen from the agreement of measured particle size distribution when represented in volume% and number%). Silver nitrate particles, c, are large, white salt crystal particles with a smooth surface morphology that looks like "wet ice bergs" when studied by SEM. The silver nitrate particles are large in size, which is also reflected by the small specific surface area, 0.03 m^2/g, measured by BET analysis.

Ag-1

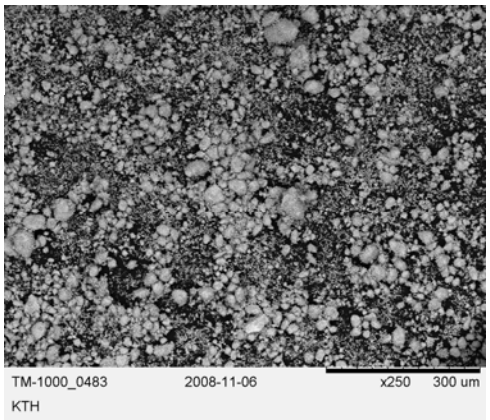

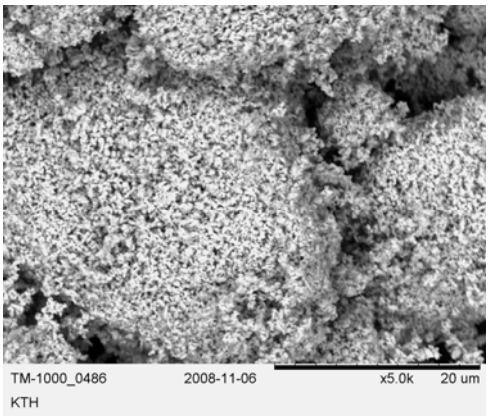

Ag_2O

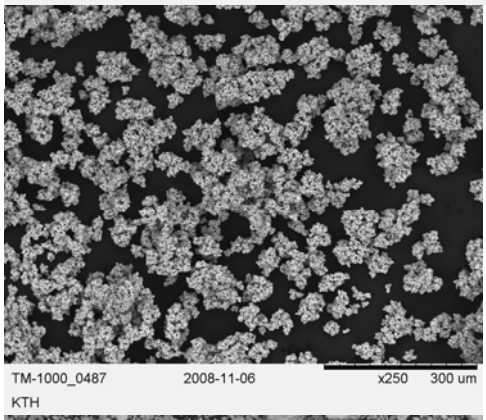

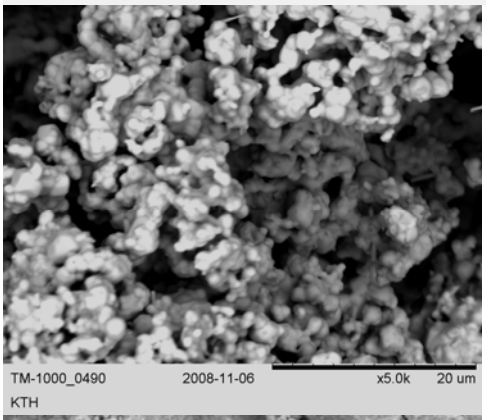

Ag-2

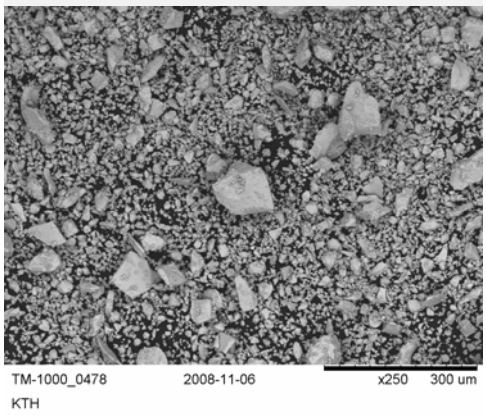

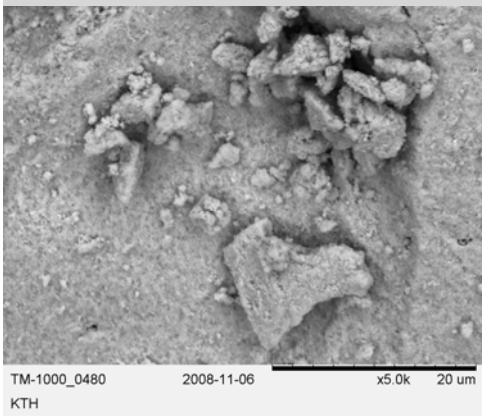

$AgNO_3$

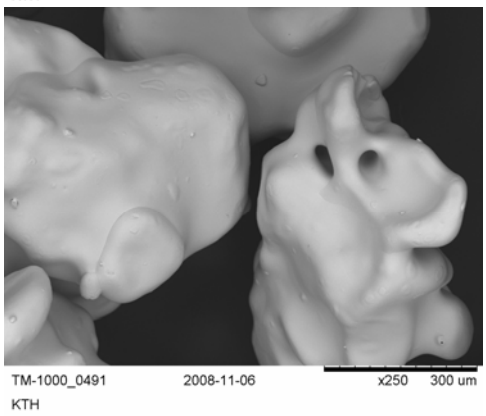

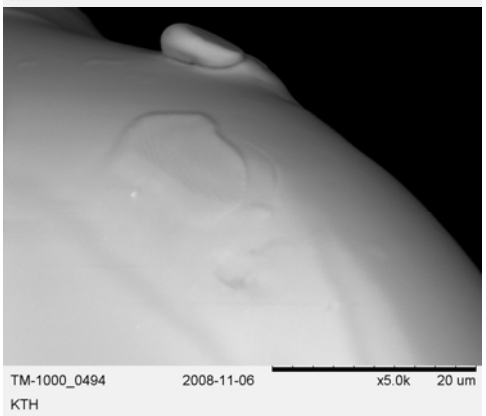

Figure 1. SEM images showing the appearance and surface morphology of silver particles, silver oxide and silver nitrate particles at magnifications of 250x and 5000x.

Table III. Measured BET specific surface area of silver metal, silver oxide and silver nitrate particles and their corresponding median particle diameter (d0.5) and the 10% (d0.1) and 90% (d0.9) size distribution cut-off points, presented as a percentage of volume (mass) and number determined from size distribution measurements in PBS using laser diffraction technique.

Test material	**BET specific surface area [m^2/g]**
Ag-1	3.1
Ag_2O	0.28
Ag-2	7.9
$AgNO_3$	0.03

Distribution volume %	**d(0.1)**	**d(0.5)**	**d(0.9)**
Ag-1	0.47 µm	8.3 µm	86.0 µm
Ag_2O	23.0 µm	43.0 µm	74.1 µm
Ag-2	19.5 µm	61.3 µm	156 µm
$AgNO_3$	18.5 µm	35.5 µm	65.8 µm

Distribution number %	**d(0.1)**	**d(0.5)**	**d(0.9)**
Ag-1	0.04 µm	0.07 µm	0.12 µm
Ag_2O	3.9 µm	5.7 µm	27.5 µm
Ag-2	2.4 µm	3.0 µm	15.6 µm
$AgNO_3$	11.7 µm	18.0 µm	32.7 µm

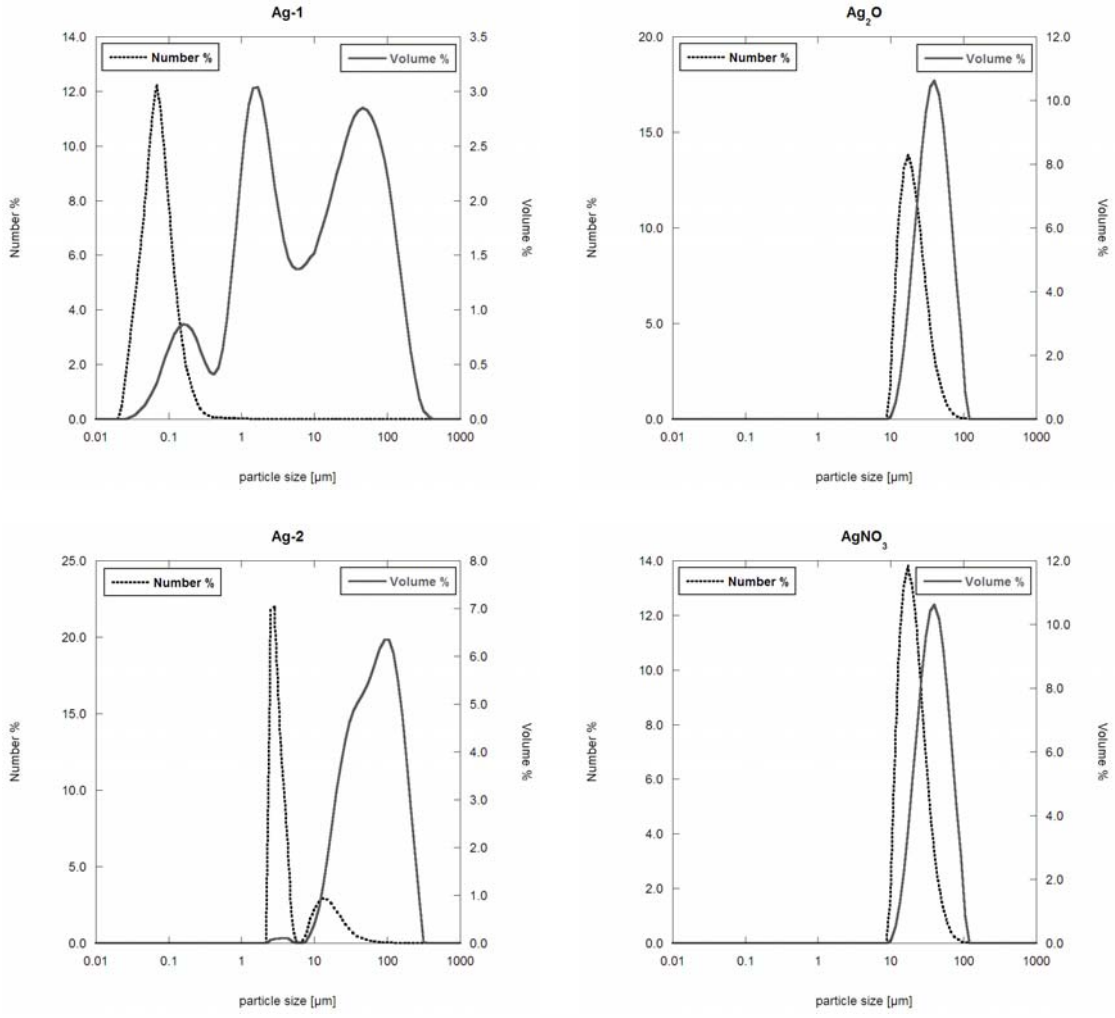

Figure 2. Particle size distributions presented as a percentage of volume (mass) and number for silver metal, silver oxide and silver nitrate particles dispersed in PBS using a laser diffraction technique.

The particle size, its size distribution, surface area, and surface morphology are all properties of particles that govern their reaction and interaction with the surrounding environment. Generally, the tendency of smaller particles to aggregate and/or to agglomerate in a given medium depends on parameters such as particle concentration, and media composition (ionic strength/salt content) (Murdock et al, 2007; He et al, 2008).

The interfacial domain between the particle and the surrounding environment acts as a site where chemical reactions can take place. Particle size and the size distribution are not only related to the surface area of the particles but also crucial for surface properties and surface reactivity. As the ratio of surface atoms to total atoms increases with decreasing particle size, the surface reactivity increases, and a larger chemical and biological activity is expected (Roduner, 2006; Oberdörster, 2005). Particles with an uneven and rough surface morphology and irregular shapes with corners and edges are more active from a chemical as well as a biological perspective. The reason for this is that edge and corner atoms have an even lower coordination (weaker bonds) to bulk atoms, and therefore bond to foreign atoms and molecules more readily (Roduner, 2006; Taylor et al, 2008).

Particle characterisation – surface composition

Typical XPS core level spectra of Ag3d, O1s, N 1s (for AgNO3) and C1s are displayed in Figures 3-6 for each test material. Duplicate or triplicate area analyses have been performed on each test material. When similar composition has been observed between the different areas investigated, only one representative detailed spectrum is presented for each element investigated ($AgNO_3$, Ag_2O), Figures 3-4. For test materials Ag-2 and Ag-1, large differences have been observed between different areas investigated, Figures 5-6. All test materials reveal adventitious carbon on the surface (285.0 eV) and small amount of oxidized carbon. A surface contamination layer of carbon is always observed to different extent due to the surface history, and its source is usually atmospheric and not possible to avoid.

The AgNO3 test material, Figure 3, shows a silver peak (Ag $3d_{5/2}$) with a binding energy of 368.6, slightly higher compared to peaks usually associated with silver oxides (368.2 eV) and in addition, peaks of nitrogen (N 1s) and oxygen (O 1s) associated with nitrate. Carbon (C 1s) is present on the surface as typical adventitious carbon due to atmospheric contamination.

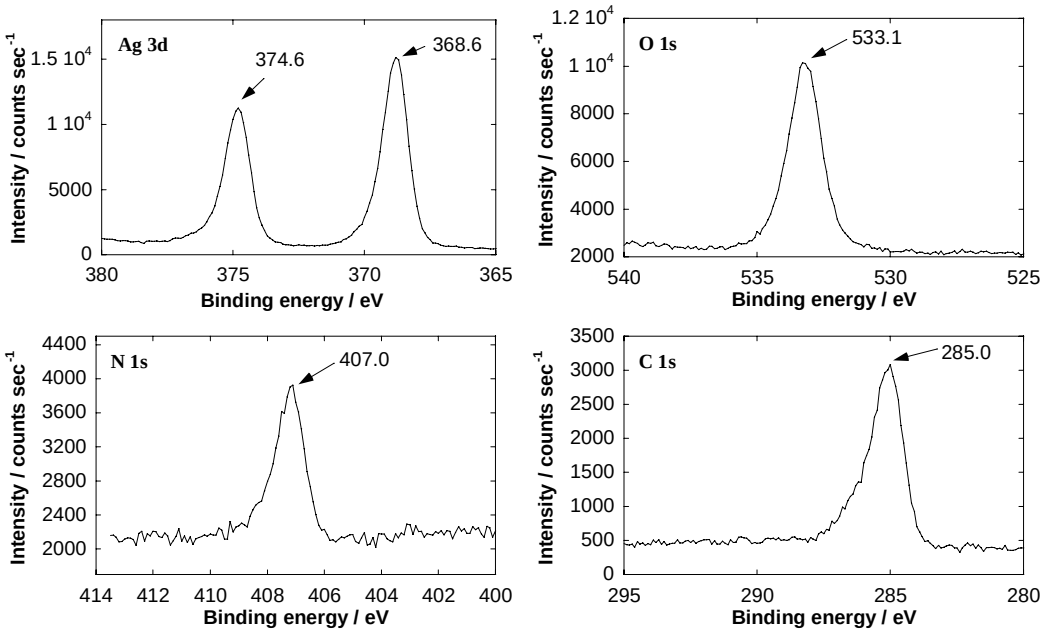

Figure 3. XPS detailed high resolution core level spectra for Ag 3d, O 1s, N 1s and C 1s of the $AgNO_3$ test material.

The Ag2O test material, Figure 4, shows a silver peak (Ag $3d_{5/2}$) with a binding energy of 368.2 eV, associated with silver oxides (Wang 1997). Both AgO and Ag_2O show closely overlapping binding energies (367.9-368.2) why no unambiguous phase identification can be made. The oxygen component (O 1s) consists of three main peaks, located at 529.7, 531.8 and 533.6 eV, respectively. These peaks are associated with silver oxide, adsorbed hydroxyl groups, and/or bulk hydroxides, respectively (Lutzenkirchen-Hecht and Strehblow, 2006; Wang 1997). Carbon (C 1s) is present on the surface as typical adventitious carbon due to atmospheric contamination.

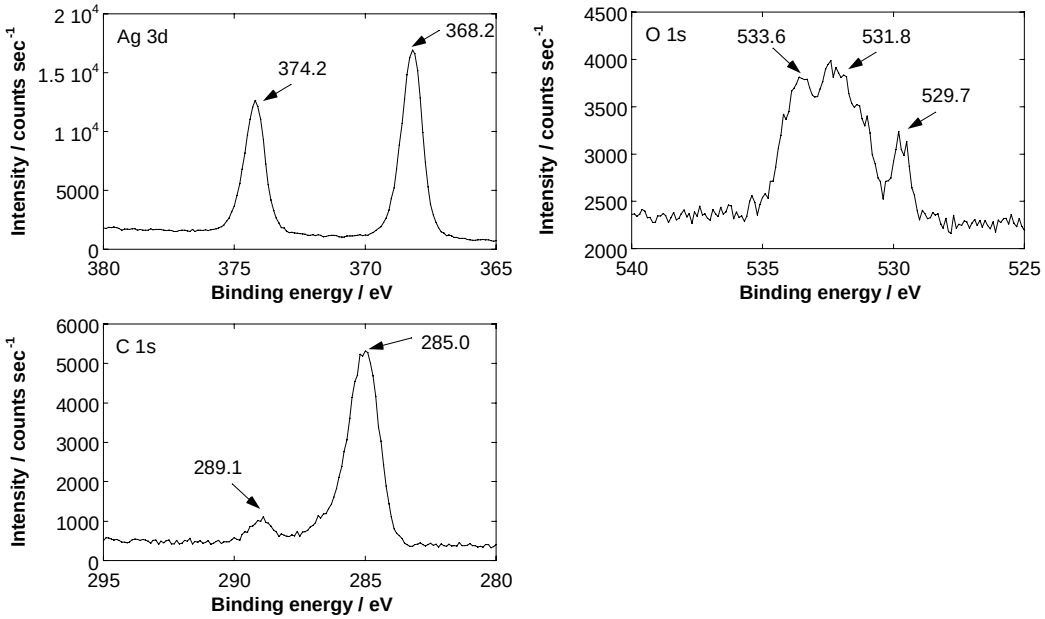

Figure 4. XPS detailed high resolution core level spectra for Ag 3d, O 1s, and C 1s of the Ag_2O test material.

The Ag-1 test material shows large variations in composition between different areas investigated, Figure 5.

Areas with silver peaks (Ag $3d_{5/2}$) with a binding energy of 368.3 eV (associated with silver oxides) were observed as well as areas with the silver peak significantly shifter to higher binding energies of 369.2-370.7 eV (Ag $3d_{5/2}$). This shift is associated to metallic silver (Wang, 1997; Lai et al 2005; Murray et al 2005; Al-Kuhaili 2007). The results imply particles with a thin surface oxide layer, or particles of varying surface coverage and thickness of the surface oxide. In addition, significant amounts of strongly oxidized carbon (carbon with single, and/or double oxygen bonding, carboxyl groups etc) of varying binding energies were detected on these particles. Their definite assignment is hazardous at this stage although it is clear that the origin is not from atmospheric contamination.

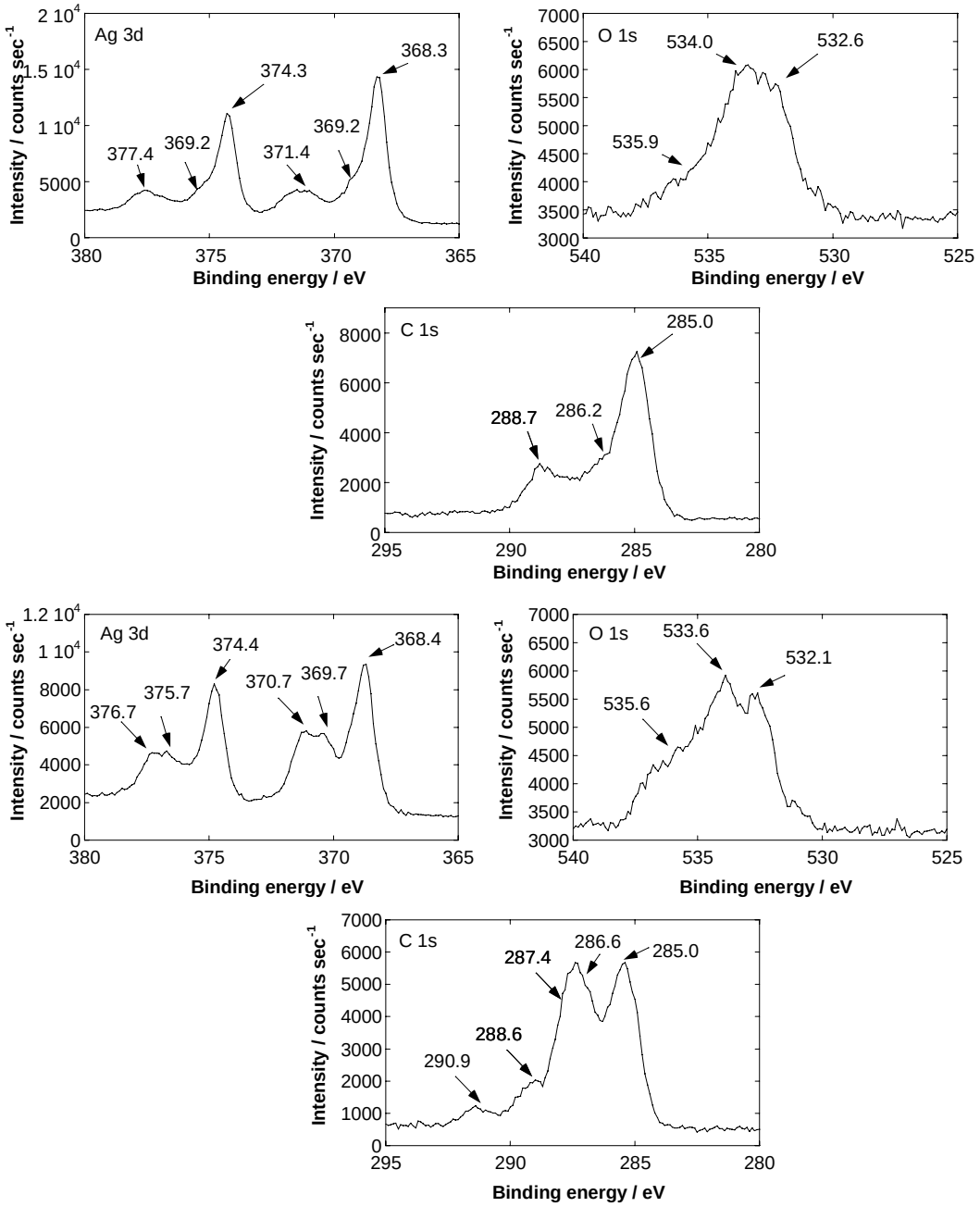

Figure 5. XPS detailed high resolution core level spectra for Ag 3d, O 1s, and C 1s at two different areas of the Ag-1 test material.

The Ag-2 test material shows large variations in composition between different areas investigated, Figure 6.

Areas with silver peaks (Ag $3d_{5/2}$) with a binding energy of 368.3 eV (most probably associated with silver oxides) were observed as well as areas with the silver peak significantly shifted to higher binding energies of 369.9-370.1 eV (Ag $3d_{5/2}$). This shifted peak is associated to metallic silver (Wang, 1997; Lai et al 2005; Murray et al 2005; Al-Kuhaili, 2007). The results imply particles with a thin surface oxide layer or particles of varying surface coverage and thickness of the surface oxide. In addition, significant amounts of strongly oxidized carbon of varying binding energies (carbon with single, and/or double oxygen bonding, carboxyl groups etc) were detected on these particles. Their definite assignment is hazardous at this stage although it is clear that the origin is not from atmospheric contamination.

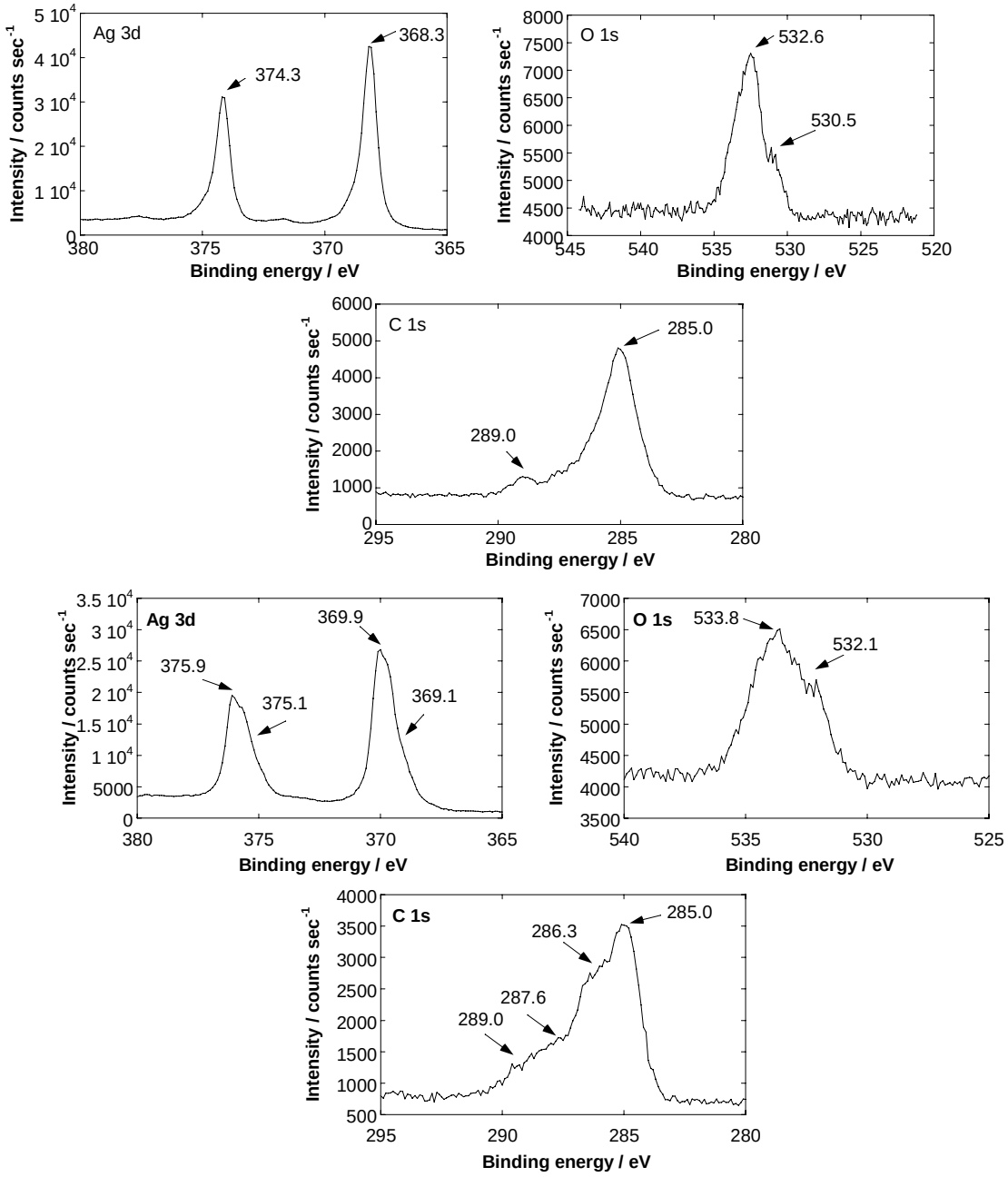

Figure 6. XPS detailed high resolution core level spectra for Ag 3d, O 1s, and C 1s at two different areas of the Ag-2 test material.

Bioaccessibility data – silver release

The concentration of silver released from the silver metal, silver oxide and silver nitrate particles after different sampling periods when exposed in the different test media are displayed in Figure 7. Error bars indicate the standard deviation of triplicate samples, and reflect in principle variations due to small differences in the amount of particles loaded in each of the three replicate samples, and also differences in surface morphology between the particles, see Figure 1. No adjustment of the solution volume to powder mass was made. The concentrations of silver that were released from the different particles were all over very similar and seem independent of material type (pure metal, oxide, nitrate). Since the concentrations measured after 2 hours and 24 hours of exposure were practically constant, it is concluded that the release/dissolution of silver takes place relatively fast and at these test conditions equilibrium is obtained during the time period prior to the 2 hour exposure and sampling. The released silver concentrations from all test materials were highest in phosphate buffered saline (PBS), having a neutral pH but the highest chloride content of the media investigated. Released silver concentrations were lowest in artificial gastric fluid (GST) with the most acidic pH and the lowest concentration of chlorides. The chloride concentration of the different test media is highest in PBS (5.35 g/L) > GMB (3.97 g/L) > ASW (3.05 g/L) > ALF (2.02 g/L) > GST (0.97g/L).

The results are in agreement with previous studies showing neutral solutions able to more strongly dissolve silver compared to alkaline conditions (Lutzenkirchen-Hecht and Strehblow, 2006).

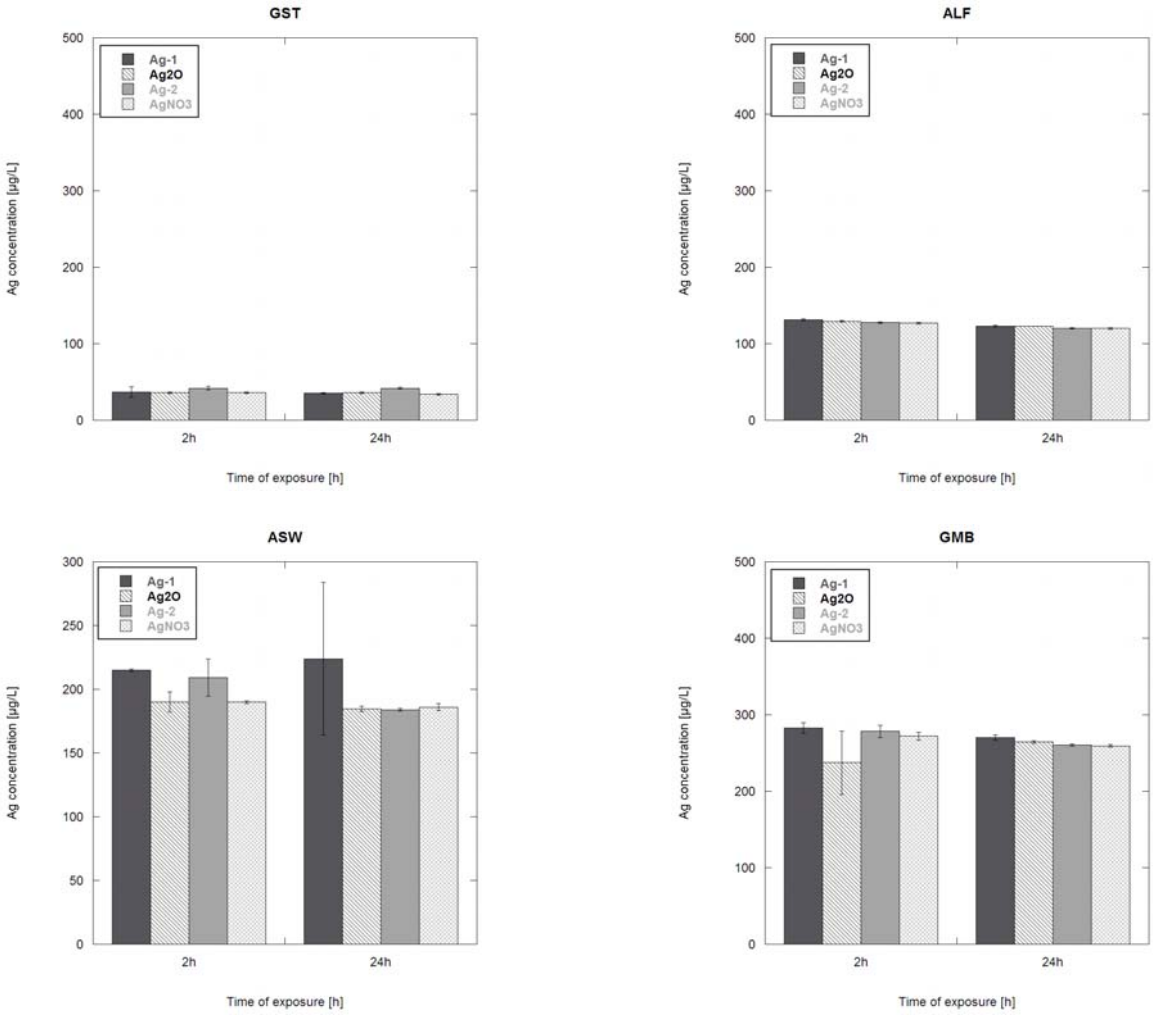

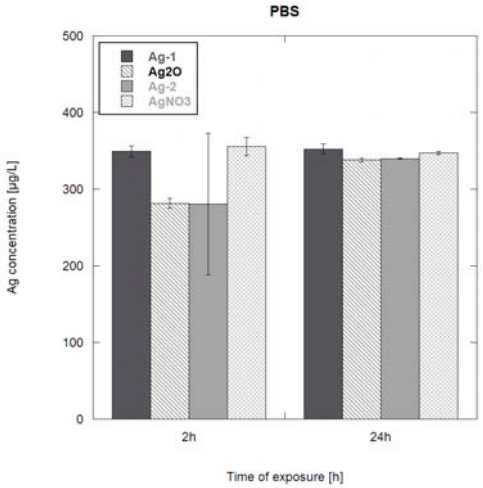

Figure 7. Released silver concentration in different test media from silver metal particles, Ag-1 and Ag-2, silver oxide, Ag_2O and silver nitrate particles, $AgNO_3$ after 2, and 24 hours of exposure. The error bars show the standard deviation of triplicate samples. Abbreviations: GST-artificial gastric fluid (pH 1.5), ALF-artificial lysosomal fluid (pH 4.5), ASW-artificial sweat (pH 6.5), GMB-Gamble´s solution (pH 7.4) and, PBS-phosphate buffered saline (pH 7.4).

Measured silver concentrations from the silver metal, silver oxide and silver nitrate particles exposed in the different synthetic media for 2 and 24 hours are compiled in Table IV.

Table IV. Total concentration of released silver [µg/L] in the different test media

Test Material	GST		ALF		ASW		GMB		PBS	
	Ag conc µg/L	Std	Ag conc µg/L	Std	Ag conc µg/L	Std	Ag conc µg/L	Std	Ag conc µg/L	Std
Ag-1 2h	36.7	6.8	131.3	1.2	215.0	1.0	282.7	6.7	349.0	7.5
Ag-1 24h	35.3	1.2	123.0	1.0	224.0	59.8	270.0	3.5	352.3	6.5
Ag_2O 2h	36.0	1.0	129.3	1.2	190.0	7.8	237.3	41.3	281.7	6.4
Ag_2O 24h	36.0	1.0	123.0	0.0	184.7	2.1	264.3	1.5	338.0	2.6
Ag-2 2h	42.0	2.6	127.7	1.2	209.3	14.6	278.3	8.1	280.7	92.2
Ag-2 24h	42.0	1.0	120.3	0.6	184.0	1.0	260.3	1.5	340.0	1.0
$AgNO_3$ 2h	36.0	1.0	127.0	1.0	190.0	1.0	272.0	5.2	355.7	11.6
$AgNO_3$ 24h	34.0	1.0	120.0	1.0	186.0	2.6	259.3	1.5	347.3	2.1

Results presented as release rates of silver per unit surface area and hour of exposure (µg/cm^2/hour), are shown in Figure 8 and compiled in Table V. These rates are calculated from the released silver concentration (Table IV) considering the solution volume, measured BET area (Table III) and sample weight (see experimental procedure), and the exposure time period. Error bars indicate the standard deviation of release rates from triplicate samples.

The silver metal, silver oxide and silver nitrate particles all show higher average release rates of silver per surface area after 2 hours exposure and lower release rates after 24 hours of exposure. In agreement to the concentration findings, the highest release rates are observed when the test materials are exposed in PBS. Since there was no kinetic behaviour observed from the measured silver concentrations, the decreasing release rates are purely an effect of the normalisation by time.
The release rate of silver decreased according to the following sequence for all samples investigated after 2 hours of exposure: PBS > GMB > ASW > ALF >> GST

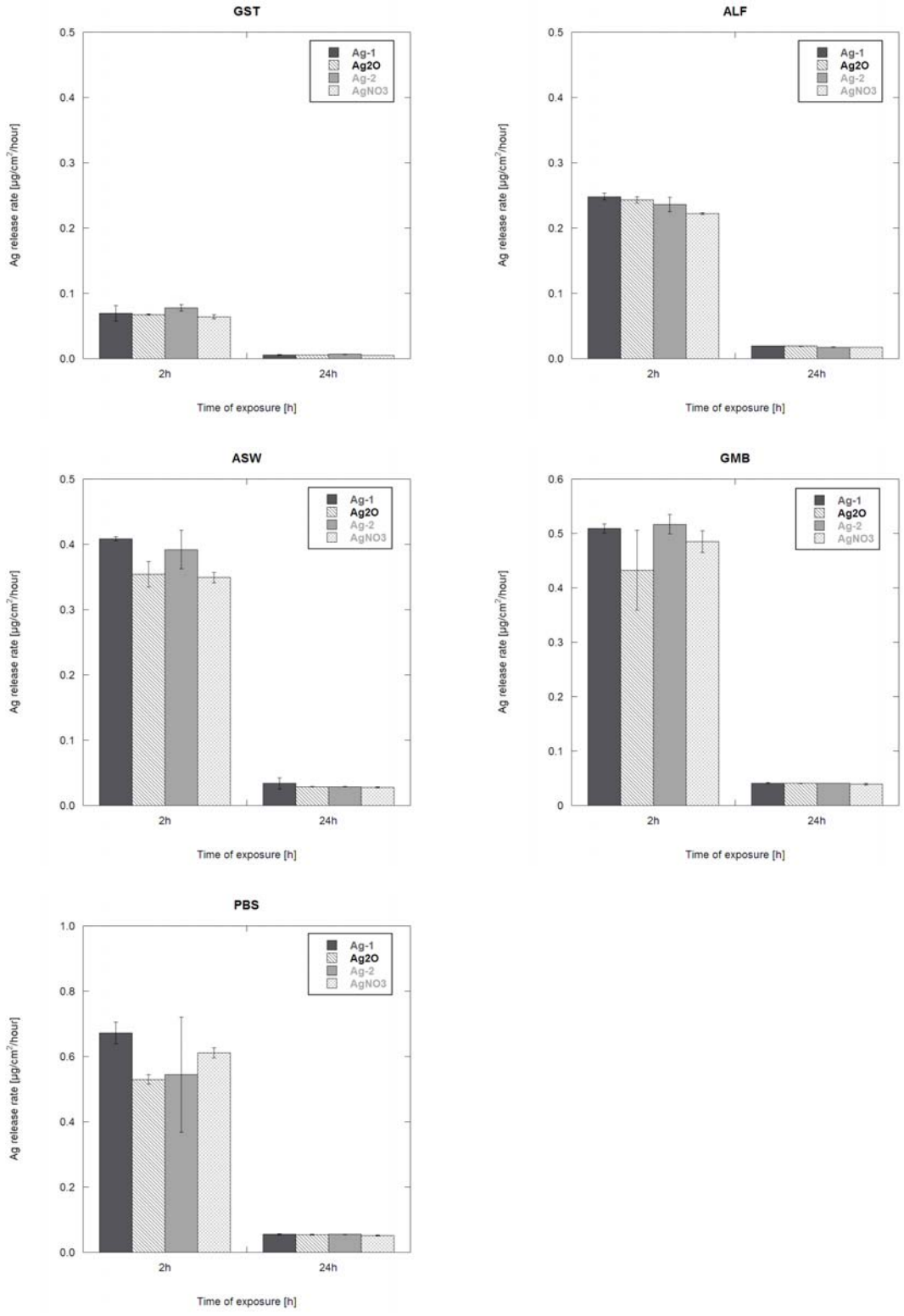

Figure 8. Release rates of silver in different test media from silver metal particles, Ag-1 and Ag-2, silver oxide, Ag_2O and silver nitrate particles, $AgNO_3$ after 2, and 24 hours of exposure. The error bars show the standard deviation of triplicate samples. Abbreviations: GST-artificial gastric fluid (pH 1.5), ALF-artificial lysosomal fluid (pH 4.5), ASW-artificial sweat (pH 6.5), GMB-Gamble´s solution (pH 7.4) and, PBS-phosphate buffered saline (pH 7.4).

Table V. Release rates of silver [µg/cm²/hour] in the different test media.

Test Material	GST		ALF		ASW		GMB		PBS	
	Ag rate µg/cm²/h	Std	Ag rate µg/cm²/h	Std	Ag rate µg/cm²/h	Std	Ag rate µg/cm²/h	Std	Ag rate µg/cm²/h	Std
Ag-1 2h	0.070	0.012	0.25	0.01	0.41	0.00	0.51	0.01	0.67	0.03
Ag-1 24h	0.006	0.000	0.02	0.00	0.03	0.01	0.04	0.00	0.06	0.00
Ag_2O 2h	0.068	0.001	0.24	0.01	0.35	0.02	0.43	0.07	0.53	0.02
Ag_2O 24h	0.006	0.000	0.02	0.00	0.03	0.00	0.04	0.00	0.05	0.00
Ag-2 2h	0.078	0.005	0.24	0.01	0.39	0.03	0.52	0.02	0.54	0.18
Ag-2 24h	0.007	0.000	0.02	0.00	0.03	0.00	0.04	0.00	0.06	0.00
$AgNO_3$ 2h	0.064	0.003	0.22	0.00	0.35	0.01	0.49	0.02	0.61	0.02
$AgNO_3$ 24h	0.005	0.000	0.02	0.00	0.03	0.00	0.04	0.00	0.05	0.00

Another comparison of release data is enabled by normalizing the released amount of silver by the amount of particles loaded for a given time period (µg/µg), Figure 9. This quotient can function as an indicative measure of the percentage of the pure metal particles that has been released (dissolved) into solution.

The results indicate that less than 0.5% of the silver metal particles have been dissolved during the 24 hours in all test media. The results are presented as the maximum percentage determined from the triplicate samples investigated to avoid underestimating the amount of dissolved silver. This conclusion could also easily be drawn based on the results of silver concentration, Figure 7.

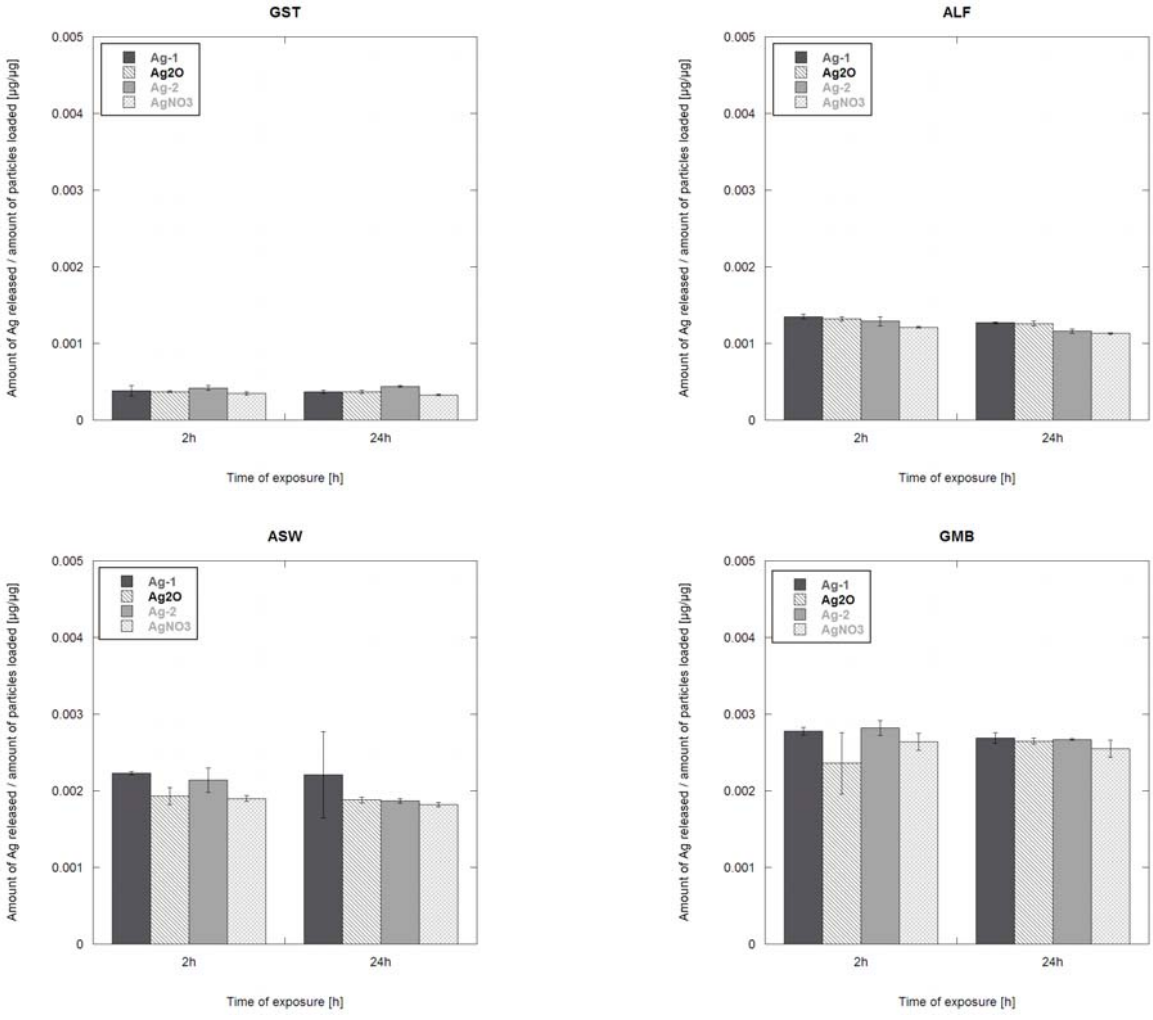

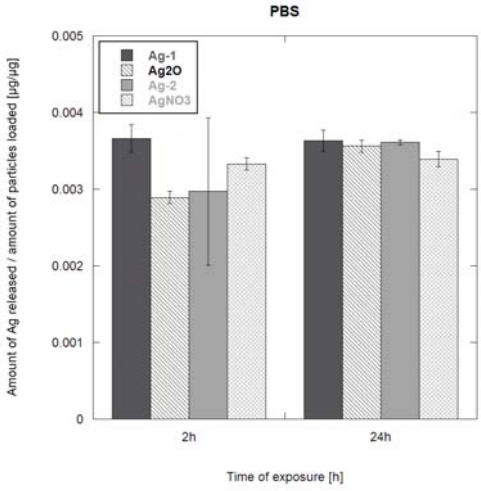

Figure 9. Released amount of silver per amount of particles loaded after exposure in different test media for 2 and 24 hours. The error bars show the standard deviation of triplicate samples. Abbreviations: GST-artificial gastric fluid (pH 1.5), ALF-artificial lysosomal fluid (pH 4.5), ASW-artificial sweat (pH 6.5), GMB-Gamble´s solution (pH 7.4) and, PBS-phosphate buffered saline (pH 7.4).

The measured amount of released silver compared to the amount of particles loaded when exposed in the different synthetic media for 2, and 24 hours are compiled in Table VI.

Table VI. Amount of released silver per amount of particles loaded [µg/µg] in the test media.

Test Material	GST		ALF		ASW		GMB		PBS	
	Ag ratio µg/µg	Std	Ag ratio µg/µg	Std	Ag ratio µg/µg	Std	Ag ratio µg/µg	Std	Ag ratio µg/µg	Std
Ag-1 2h	0.0004	0.0001	0.0014	0.0000	0.0022	0.0000	0.0028	0.0000	0.0037	0.0002
Ag-1 24h	0.0004	0.0000	0.0013	0.0000	0.0022	0.0006	0.0027	0.0001	0.0036	0.0001
Ag_2O 2h	0.0004	0.0000	0.0013	0.0000	0.0019	0.0001	0.0024	0.0004	0.0029	0.0001
Ag_2O 24h	0.0004	0.0000	0.0013	0.0000	0.0019	0.0000	0.0026	0.0000	0.0036	0.0001
Ag-2 2h	0.0004	0.0000	0.0013	0.0001	0.0021	0.0002	0.0028	0.0001	0.0030	0.0010
Ag-2 24h	0.0004	0.0000	0.0012	0.0000	0.0019	0.0000	0.0027	0.0000	0.0036	0.0000
$AgNO_3$ 2h	0.0003	0.0000	0.0012	0.0000	0.0019	0.0000	0.0026	0.0001	0.0033	0.0001
$AgNO_3$ 24h	0.0003	0.0000	0.0011	0.0000	0.0018	0.0000	0.0026	0.0001	0.0034	0.0001

Exposures of the silver metal, silver oxide and silver nitrate particles in the various media resulted in similar changes in pH with increasing time of exposure between the blank sample (media without any particles) and the triplicate samples (with particles). The maximum variations in pH of the test media upon exposure (2-24 hours) are compiled in Table VII. Generally, variations in pH between the blank sample and the triplicate samples are very similar except for artificial sweat where the silver oxide particles caused an increase in pH instead of a decrease that was observed for the other test materials and blank samples. Observed changes in pH for all the test media are within the normal range based on previous experience from this type of metal release exposures. An increasing pH upon exposure in ASW could be related to the formation of $Ag(NH_3)_2^+$, known to form in ammonium containing media.

Table VII. Maximum variations in pH of each test media upon exposure (2 and 24 hours) without (blank), or with (sample), particles. A (+) sign indicates an increase in pH, and a (–) sign a decreasing pH upon exposure. Abbreviations: GST-artificial gastric fluid (pH 1.5), ALF-artificial lysosomal fluid (pH 4.5), ASW-artificial sweat (pH 6.5), GMB-Gamble´s solution (pH 7.4) and, PBS-phosphate buffered saline (pH 7.4).

Test media	Blank	Sample
GST	- 0.22	- 0.22
ALF	- 0.08	- 0.06
ASW	-0.84	- 0.92 (+ 1.57 for Ag_2O)
GMB	+ 1.31	+ 1.38
PBS	+ 0.03	+ 0.13

References

ASTM D5517-03 (2003) "Standard test method for determining extractability of metals from art materials"

M.F. Al-Kuhaili, Journal of Physics D: Applied Physics, 40, 2847-2853, (2007), "Characterization of thin films produced by the thermal evaporation of silver oxide"

I. Balashazy, A. Farkas, I Szoke, W. Hofmann, R. Sturm, Radiation Protection Dosimetry 105 (1-4), 129-132, (2003) "Simulation of deposition and clearance of inhaled particles in central human airways"

European standard, "Test method for release of nickel from products intended to come into direct and prolonged contact with the skin", EN 1811 (1998)

S. C. Hamel, B. Buckley, P. J. Lioy, Environmental Science and Technology 32(3), 358-362, (1998), "Bioaccessibility if Metals in Soils for Different Liquid to Solid Ratios in Synthetic Gastric Fluid"

T. Hanawa, Materials Science and Engineering: C, 24,745-752, (2004), "Metal ion release from metal implants"

Y. T. He, J. Wan, T. Tokunaga, Journal of Nanoparticle Research, 10, 321 (2008), "Kinetic stability of hematite nanoparticles: the effect of particle sizes"

G. Herting, I. Odnevall Wallinder, C. Leygraf, Corrosion Science 48, 2120-2132, (2006a), "Factors that influence the release of metals from stainless steels exposed to physiological media"

G. Herting, I. Odnevall Wallinder and C. Leygraf, Corrosion Science 49, 103-111, (2006b), "Metal release from various grades of stainless steel exposed to synthetic body fluids"

A.T. Kuhn, T. Rae, in P.E. Francis, T.S. Lee (Eds), "The use of Synthetic Environments for Corrosion Testing", ASTM STP 970, American Society for Testing and Materials, Philadelphia 79-97, (1988), "Synthetic environments for the testing of metallic biomaterials"

X. Lai, T.P. St.Clair, D. W. Goodman, Faraday Discussusions, 114, 279 – 284 (1999), "Oxygen-induced morphological changes of Ag nanoclusters supported on TiO_2(110)"

D. Lutzenkirchen-Hecht, H.H. Strehblow, Surface and Interface Analysis, 38, 686-690 (2006), "The anodic oxidation of silver in 1M NaOH: electrochemistry, ex. situ XPS and in situ X-ray absorption spectroscopy"

T.B. Martonen, Z. Zhang, Y.Yang, Journal of Aerosol Science 23(4), 389-406, (1992a),"Interspecies modelling of inhaled particle deposition patterns"

T.B. Martonen, Z. Zhang, Y.Yang, Inhalation Toxicology 4(4), 303-324 (1992b),"Extrapolation modelling of aerosol deposition in human and laboratory rat lungs"

K. Midander, I. Odnevall Wallinder, C. Leygraf, Environmental Pollution 145, 51-59(2007), "In vitro studies of copper release from powder particles in synthetic biological media"

K. Midander, J. Pan, C. Leygraf, Corrosion Science 48, 2855-2866 (2006). "Elaboration of test method for the study of metal release from stainless steel particles in artificial biological media"

M. Miki, T. Isawa, T. Teshima, Y. Anazawa, M Motomiya, Nuclear Medicine communications 13(7) 553-562 (1992) "Difference in inhaled aerosol deposition patterns in the lungs due to three different sized aerosols"

O.R. Moss, Journal of Health Physics Society 36 (1979) 447, "Simulants of lung interstitial fluid"

R. C. Murdock, L. Braydich-Stolle, A. M. Schrand, J. J. Schlager, S. M. Hussain, Toxicological Science, 239-253 (2007), "Characterization of nanomaterial dispersion in solution prior to in vitro exposure using dynamic light scattering technique".

B. J. Murray, Q. Li, J. T. Newberg, E. J. Menke, J. C. Hemminger, R. M. Penner, Nano Letter, 5(11), 2319-2324 (2005), "Shape- and Size-Selective Electrochemical Synthesis of Dispersed Silver(I) Oxide Colloids"

A. Norlin, J. Pan, C. Leygraf, Biomolecular Engineering, 19, 67-71 (2002), "Investigation of interfacial capacitance of Pt, Ti and TiN-coated electrodes by electrochemical impedance spectroscopy"

G. Oberdorster, E. Oberdorster, J. Oberdorster, Environmental Health Perspective, 113, 823 – 839 (2005) "Nanotoxicology: An emerging discipline evolving from studies of ultrafine particles"

Y.Okazaki, E. Gotoh, Biomaterials, 26 (1), 11-21 (2005), "Comparison of metal release from various metallic biomaterials in vitro"

E. Roduner, Chemical Society Review, 35, 583-592 (2006), "Size matters: why nanomaterials are different"

W. Stopford, J. Turner, D. Cappelini, T. Brock, Journal of Environmental Monitoring 5 (2004) 675-680, "Bioaccessibility testing of cobalt compounds"

C. D. Taylor, M. Neurock, J. R. Scully, Journal of Electrochemical Society, 155, C407-C414 (2008), "First-principles investigation of the fundamental corrosion properties of a model Cu_{38} nanoparticle and the (111), (113) surfaces"

P.W. Wang, Materials Chemistry and Physics, 50, 213-218 (1997), "Thermal activation energy of silver in ion-exchanged soda-lime glass investigated by X-ray photoelectron spectroscopy"